Annually resolved δ^2H tree-ring chronology of the lignin methoxyl groups from Germany reflects averaged Western European surface air temperature changes

Anhäuser, Tobias[1*]; Sehls, Birgit[1]; Thomas, Werner[2]; Hartl, Claudia[3]; Greule, Markus[1];
Scholz, Denis[4], Esper, Jan[3] and Keppler, Frank[1,5*]

[1]Institute of Earth Sciences, Heidelberg University, Im Neuenheimer Feld 236, D-69120 Heidelberg, Germany
[2]Deutscher Wetterdienst, Meteorological Observatory station Hohenpeißenberg, Germany, Albin-Schwaiger-Weg 10, D-82383 Hohenpeissenberg, Germany
[3]Department of Geography, Johannes Gutenberg University of Mainz, Johann-Joachim-Becher-Weg 21, 55128 Mainz, Germany
[4]Institute of Geosciences, Johannes Gutenberg University of Mainz, Germany, Johann-Joachim-Becher-Weg 21, D-55128 Mainz, Germany
[5]Heidelberg Center for the Environment HCE, Heidelberg University, D-69120 Heidelberg, Germany

*Correspondence to: Tobias Anhäuser (tobias.anhaeuser@geow.uni-heidelberg.de) and Frank Keppler (frank.keppler@geow.uni-heidelberg.de)

Abstract. Stable hydrogen isotopes ratios of lignin methoxyl groups (expressed as δ^2H$_{LM}$) of wood have been shown to reflect the climate-sensitive δ^2H values of precipitation (expressed as δ^2H$_{precip}$) modulated by a large uniform negative isotope fractionation. However, a detailed calibration study among temporal variabilities of δ^2H$_{LM}$ in tree-ring series, site-specific δ^2H$_{precip}$ and climate parameters has not been performed yet. Here, we present annually resolved δ^2H$_{LM}$ values from nine tree-ring series (derived from four *Fagus sylvatica* L. trees) collected near stations of the Global Isotope Network of Isotopes in Precipitation (GNIP) and the Deutsche Wetterdienst (DWD) meteorological observatory at Hohenpeißenberg (southern Germany; ~48°N, 11°E). The measured nine δ^2H$_{LM}$ tree-ring series (common period of overlap 1916-2015) show a strong coherency as indicated by highly significant ($p<0.001$) inter-series correlations (mean value Rbar = 0.52) and no indication of any known (stable isotope-specific) juvenile trend affecting the first decades of growth. When compared to local instrumental data, the combined δ^2H$_{LM}$ chronology shows highest correlations with annually averaged data of δ^2H$_{precip}$ as well as temperature particularly when using the year defined from previous September to current August (r = 0.73 and 0.56, respectively, $p<0.001$). However, the Hohenpeißenberg δ^2H$_{LM}$ chronology shows enhanced correlations with land and sea surface air temperature for multiple (broadly combined) areas across Western Europe (r > 0.6, $p<0.1$). We subsequently established a linear regression model between averaged Western European surface air temperatures (range: 30°W–20°E, 35–60°N) and the δ^2H$_{LM}$ chronology (r = 0.71, $p<0.001$). When comparing instrumental and reconstructed large-scale temperature anomalies from the year 1916 to 2015, an average absolute deviation in annual reconstructions of as low as 0.3 °C was found (n = 100). Therefore, δ^2H$_{LM}$ values of mid-latitudinal tree-ring archives are considered suitable for large-scale mean annual temperature reconstructions and are therefore able to improve the paleoclimatic potential of Late Holocene tree-ring archives.

Climate
of the Past

Discussions

Open Access

EGU

1. Introduction

High-resolution tree-ring series are valuable climate archives, ~~particularly for the Late Holocene,~~ fundamentally

45   contributing to the understanding of past and current climate variability (Büntgen et al., 2011; Esper et al., 2002; Mann et al., 1998). Dendrochronological climate proxies are commonly used to reconstruct local temperature variability derived from ~~plant~~ physiological parameters, such as tree-ring width (TRW) or maximum late wood density (MXD) from trees growing at or close to the altitudinal or latitudinal treeline. Alternative proxies potentially suitable for climate reconstructions of non-treeline regions are tree-ring stable hydrogen and oxygen

50   isotope ratios (expressed as δ^2H and $\delta^{18}O$ values) of stem wood as they reflect ~~partly~~ stable water isotopes of the local precipitation (δ^2H_{precip} and $\delta^{18}O_{precip}$) (Hartl-Meier et al., 2014; Liu et al., 2015; McCarroll and Loader, 2004; Pauly et al., 2018; Sternberg, 2009; Treydte et al., 2006). Both δ^2H and $\delta^{18}O$ values are sensitive tracers of hydroclimate as they integrate a combination of (i) meteorological conditions in the moisture source area, (ii) changes during the meridional atmospheric vapor transport (particularly water volume loss, but also potential

55   mixing of different air masses), and (iii) local temperature (Araguas-Araguas et al., 2000; Dansgaard, 1964; Rozanski et al., 1993). Hence, reconstructions of δ^2H_{precip} and $\delta^{18}O_{precip}$ values are not only able to broaden the applicability of tree-ring archives for non-treeline regions, but may also complement commonly used tree-ring proxies ~~(reflecting local climate changes)~~ with an additional stable isotope proxy ~~(reflecting local and large-scale hydroclimatic changes)~~.

60   The compound of choice for paleoclimate investigation is commonly cellulose since their stable oxygen and hydrogen isotopes signatures are derived from the climate-sensitive stable water isotopes. However, cellulose incorporates hydrogen and oxygen atoms partly from leaf-water that experienced an evaporative ^2H and ^{18}O enrichment prior to biosynthesis potentially complicating the reconstruction of the initial source water δ^2H and $\delta^{18}O$ values (Flanagan et al., 1991; Roden et al., 2000). Furthermore, the extraction procedures are time

65   consuming. Thus, studies are commonly forced to pool samples or build chronologies using only low or even no replication hampering the statistical evaluation of the accompanied δ^2H and $\delta^{18}O$ variability in high resolution tree-ring series (McCarroll and Loader, 2004).

Another wood component that has been increasingly employed for the investigation of δ^2H values in tree-ring series are lignin methoxyl groups (expressed as δ^2H_{LM} values). Methoxyl groups (R-OCH_3) in wood are

70   predominantly ether bonded in lignin including three non-exchangeable hydrogen atoms that do not exchange with other hydrogen containing organic compounds or surrounding water. Hence, contrary to the cellulose-derived δ^2H values, δ^2H_{LM} values are not influenced by an evaporative ^2H enrichment of leaf water since the wood component lignin is formed within the xylem tissue. Furthermore, δ^2H_{LM} values of wood can readily be measured as methyl iodide (CH_3I) upon treatment with hydroiodic acid providing a fast and straightforward

75   extraction method. Earlier studies mainly evaluated and quantified the spatial δ^2H_{precip}-δ^2H_{LM} relationship using numerous sampling sites (Anhäuser et al., 2017a; Feakins et al., 2013; Keppler et al., 2007), but also investigated site-specific δ^2H_{LM} variabilities between trees at single sites (Anhäuser et al., 2017b). These studies suggest δ^2H_{LM} values reflect δ^2H values of the tree's source water (δ^2H_{sw} values) as significant relationships between

$\delta^2 H_{LM}$ and mean annual $\delta^2 H_{precip}$ values could be observed (implying that $\delta^2 H_{sw}$ values reflects an annual integral

80   of the site-specific $\delta^2 H_{precip}$ value). As $\delta^2 H_{sw}$ values were not measured in most of these studies, the estimated isotope fractionation was calculated between $\delta^2 H_{precip}$ and $\delta^2 H_{LM}$ (commonly expressed as the apparent isotope fractionation ε_{app}) and is considered to reflect primarily the biosynthetic isotope fractionation (ε_{bio}) during lignin methoxyl biosynthesis.

Calculations of ε_{app} showed a broad agreement between coniferous and deciduous tree-species (n = 13) with ε_{app}

85   values of –213 ± 17 ‰ except for *Picea abies* (–237 ± 19 ‰; Anhäuser et al., 2017a). At a single site, $\delta^2 H_{LM}$ values showed maximum differences of ≤ 28 ‰ between five trees (within a circumference of 200 m). Hence, the accompanied variability of ε_{app} (in the range of ± 17 to 19 ‰) was mainly assigned to inter-tree variability and defines (at this stage of research) the accuracy to reconstruct 'absolute' $\delta^2 H_{precip}$ values using $\delta^2 H_{LM}$ values. Reconstructions of 'absolute' $\delta^2 H_{precip}$ values have therefore been considered suitable for when performed on

90   wood samples covering anticipated large $\delta^2 H_{precip}$ changes (exceeding the accompanied ε_{app} variability of ± 17 to 19 ‰) as could recently been shown for deep-time Eocene fossil wood specimen (Anhäuser et al., 2018).

Anhäuser et al. (2017a) suggested that relative temporal $\delta^2 H_{LM}$ changes, measured from multiple tree-ring series, may reflect relative temporal $\delta^2 H_{precip}$ changes much more accurately since the characterized main noise of ε_{app} (inter-tree variability) is minimized. Earlier studies conducted preliminary investigations of inter-annually

95   resolved $\delta^2 H_{LM}$ tree-ring series (Gori et al., 2013; Mischel et al., 2015; Riechelmann et al., 2017). However, a detailed evaluation of the temporal $\delta^2 H_{LM}$-$\delta^2 H_{precip}$ relationship was not possible either due to lacking site-specific instrumental $\delta^2 H_{precip}$ data (Gori et al., 2013; Mischel et al., 2015; Riechelmann et al., 2017) or potentially insufficient tree-ring series length of two decades (Mischel et al., 2015). Furthermore, Gori et al. (2013) and Riechelmann et al. (2017) used trees growing predominantly on thin soils and steep slopes as

100   sampling was carried out in mid- to high-altitudinal Alpine regions (~900, ~1300, ~1500 and ~1900 m.a.s.l.). At such sites, tree source water is considered prone to $\delta^2 H$ changes due to a low residence time and capacity of soil water leading to seasonally biased soil water accumulation.

To evaluate in detail the significance of $\delta^2 H_{LM}$ to reflect $\delta^2 H_{precip}$ and its potential for climate reconstructions, this study investigates tree-ring $\delta^2 H_{LM}$ variability in the vicinity (< 2 km) of stations of the Global Network of

105   Isotopes in Precipitation (GNIP) and the Deutsche Wetterdienst (DWD) located at Hohenpeißenberg (Germany). Nine cores from four *Fagus sylvatica* L. specimens were used to perform inter-annually resolved $\delta^2 H_{LM}$ measurements with a common period of overlap 1916-2015. The data are used to assess the co-variance among radii and different trees and to evaluate potential non-climatic age-related influences. Subsequently, the $\delta^2 H_{LM}$ tree-ring series are compared to site-specific $\delta^2 H_{precip}$ reference data as well as local and large-scale climate data.

110   **2. Study site and local climate**

The study was conducted around the Hoher Peißenberg Mountain near the Hohenpeißenberg municipality in the northern Alpine foothills in Germany (47° 48' N, 11° 01' E; ~800 m.a.s.l.; Fig. 1). Mean annual temperatures (MAT) during the 1916-2015 period ranged from 4.8 to 8.5 °C with a mean value of 6.6 °C and monthly temperatures varying between –1.4 °C (January) and 15.2 °C (July) (Fig. 2a,b). For the same time period, total

115   annual precipitation ranged between 780 and 1570 mm averaging 1160 mm, whereby half of the total annual precipitation falls between May and August. Monthly resolved $\delta^2 H_{precip}$ data are available from 1971-2008 from the nearby GNIP station (Fig. 2c, d). Weighted mean annual $\delta^2 H_{precip}$ values show an average value of –75 ‰

Climate
of the Past
Discussions

with a seasonal range from −107 (February) to −52 ‰ (August). Long-term climate trends of the 1916-2015
120   period at Hohenpeißenberg show that MATs increased significantly by 0.12 °C per decade (r = 0.56, p < 0.001),
whereby neither significant changes in annual nor seasonal precipitation are observed (considering
meteorological seasons). For the 1971-2008 period, weighted mean annual $\delta^2 H_{precip}$ values correlate highly
significantly with MAT (r = 0.52, p < 0.001), but show neither a significant correlation with annual precipitation
(r = −0.05, p = 0.62) nor with seasonal precipitation (r ranging from −0.32 to 0.2, p > 0.05).

3. Material and methods

125   ### 3.1 Tree-ring material

Twenty *F. sylvatica* trees were sampled in spring and autumn 2016 at Hohenpeißenberg. We took two to three
cores per tree at breast height (~1.2 m above ground) with a 5-mm increment borer yielding a total number of 52
cores (core lengths ranged from 400 to 600 mm). The four *Fagus sylvatica* trees (referred to as F1, F2, F3 and
F4; cf. Fig. 1) selected for $\delta^2 H_{LM}$ measurements were either located at moderate east-facing slopes (< 10%), such
130   as F1 and F2, or in flat terrain, such as F3 and F4.

After collection, increment cores were cut perpendicular to the wood fibers using a core-microtome to ease ring
identification (Gärtner and Nievergelt, 2010). Tree-ring width (TRW) was measured for all cores with an
accuracy of 0.01 mm using a LINTAB measuring table equipped with TSAP-Win Software (both Rinntech,
Heidelberg, Germany). Cross-dating accuracy was assessed visually and statistically using the program
135   COFECHA (Holmes, 1983). For $\delta^2 H_{LM}$ analysis, four trees (F1 to F4) with no obvious disturbance influence, i.e.
growth release or suppression, were selected. To better assess intra-tree variability we choose three cores of F1
and two cores of F2, F3 and F4 (termed F1.1, F1.2, F1.3 and so on, Table 1). The longest tree-ring series of the
four *Fagus sylvatica* trees date back to 1905 (F1.2), 1844 (F2.2), 1890 (F3.1) and 1896 (F4.1) and were used to
determine the 'pith offset' (number of missing innermost rings). The corresponding shortest tree-ring series for
140   each tree dated back to 1912 (both F1.1 and F1.3), 1858 (F2.1), 1916 (F3.2) and 1916 (F4.2). Consequently,
each *Fagus sylvatica* tree provides a minimum of two radii that covered the 1916-2015 common period whereby
two radii older than 1916 are particularly provided by F2 (extending back to 1844 and 1858). Over the full
periods, tree rings were carefully dissected at the tree ring border (latewood/earlywood transition) with a scalpel
under a magnifier to subsequently allow annually resolved $\delta^2 H_{LM}$ measurements. All dissected tree-ring samples
145   yielded a minimum weight of 1 mg.

3.2 Instrumentation and analytical uncertainty of $\delta^2 H_{LM}$ analysis

The $\delta^2 H_{LM}$ value of wood can be measured as CH_3I released upon treatment of the samples with hydroiodic acid
(HI) by the method described by Greule et al. (2008). Briefly, HI (0.25 ml; puriss. p.a., 55-60%, not stabilized,
150   purchased from Sigma-Aldrich, Seelze, Germany, or Gillingham, UK, respectively) was added to the annually
dissected tree-rings (1 to 10 mg, not homogenized) in a crimp glass vial (1.5 ml; IVA Analysentechnik,
Meerbusch, Germany). The vials were sealed with crimp caps containing PTFE lined butyl rubber septa
(thickness 0.9mm) and incubated for 30 minutes at 130°C. After heating, the samples were subsequently allowed
to equilibrate at room temperature (22 ± 0.5 °C, air conditioned room) for at least 30 minutes before an aliquot of

Climate
of the Past

Discussions

155   the headspace (10-90 µl) was collected and directly injected into the analytical system using a gastight syringe
(100 µl, SGE Analytical Science).

δ^2H values of the CH$_3$I formed from the methoxyl groups in the wood samples (δ^2H$_{LM}$) were measured using an
HP 6890N gas chromatograph (Agilent, Santa Clara, USA) equipped with an auto sampler A200S (CTC
Analytics, Zwingen, Switzerland), coupled to a Delta^{PLUS}XL isotope ratio mass spectrometer (ThermoQuest

160   Finnigan, Bremen, Germany) via a thermo conversion reactor [ceramic tube (Al$_2$O$_3$), length 320 mm, 0.5 mm
i.d., reactor temperature 1450 °C] and a GC Combustion III Interface (ThermoQuest Finnigan, Bremen,
Germany). The gas chromatograph (GC) was fitted with a Zebron ZB-5MS capillary column (Phenomenex,
Torrance, USA) (30m x 0.25mm i.d., d$_f$ 1µm), and the following conditions were employed: split injection (4:1),
initial oven temperature at 30 °C for 3.8 min, ramp at 30 °C/min to 100 °C. Helium was used as carrier gas at a

165   constant flow rate of 0.6 mL/min.

A tank of high purity hydrogen gas (H$_2$, hydrogen 5.0, Linde, Höllriegelskreuth, Germany) with a δ^2H value
ranging from –195 to –225 ‰ (vs. V-SMOW, range provided by the supplier) was used as the working reference
gas. The H$_3^+$ factor, determined daily during the measurement period, was between 1.9 and 2.4 ppm/nA.

All δ^2H$_{LM}$ values were normalized by a two-point linear calibration (Paul et al., 2007) using δ^2H values of two

170   CH$_3$I working standards relative to V-SMOW. The δ^2H values of the CH$_3$I working standards were calibrated
against international reference substances (VSMOW2 [δ^2H$_{VSMOW}$ = 0.0 ± 0.3 ‰] and SLAP2 [δ^2H$_{VSMOW}$ =
−427.5 ± 0.3 ‰]) using TC/EA-IRMS (elemental analyser-isotopic ratio mass spectrometer IsoLab, Max Planck
Institute for Biogeochemistry, Jena, Germany). The calibrated δ^2H values in ‰ versus V-SMOW for the two
CH$_3$I working standards were −173.0 ± 1.5 ‰ (n=9, 1σ) and −66.2 ‰ ± 1.2 ‰ (n=8, 1σ). All samples were

175   measured in triplicate followed by consecutive injections of both working standards. Standard deviations (1σ) of
the triplicate measurements averaged ± 1.4 ‰ (ranging from < ± 0.1 to 13.9 ‰). Additional uncertainty is
introduced by the 'external precision' (also referred as the chemical replication uncertainty). To estimate this
uncertainty, we cut tree rings (n = 68) parallel to growth direction to obtain three tree-ring subsamples of the
same cambial age (each comprising early and late wood). These subsamples enabled three separate HI treatments

180   and subsequent δ^2H$_{LM}$ analysis. The standard deviation of the three subsamples (n = 68) averaged ± 2.7 ‰ (1σ)
and was used as estimator for the 'external precision'. Using Gaussian error propagation, the overall analytical
uncertainty of the δ^2H$_{LM}$ determination averaged ± 3.6 ‰ (ranging from ± 3.3 to ± 14.4 ‰ with n = 1086).

3.3 δ^2H$_{LM}$ covariance assessment and calibration

Coherency among the nine δ^2H$_{LM}$ tree-ring series was assessed over the 1916-2015 common period using

185   Pearson's correlation coefficient (r) as well as the inter-series correlation (Rbar). To identify potential non-
climatic trends of δ^2H$_{LM}$ values of juvenile tree-rings, we compared linear trends among differently old trees
over a common time period. First year autocorrelation (lag-1) has been calculated to determine the influence of
the previous year on δ^2H$_{LM}$.

Since tree-ring δ^2H$_{LM}$ is primarily derived from δ^2H$_{precip}$, we firstly calculated Pearson's correlation coefficients

190   from 1971-2008 between these data using a variety of monthly, seasonal and annual mean values to evaluate the
tree´s source water. Moreover, tree source water can - to some extent - involve the precipitation of the previous
year (Ehleringer and Dawson, 1992; Feng and Epstein, 1995; Tang et al., 2000). Hence, we also included
δ^2H$_{precip}$ signatures of months of the preceding fall as well as 'shifted' annual values, such as previous September

Climate
of the Past
Discussions

to current August. Whenever δ^2H_{precip} values were averaged, individual δ^2H_{precip} values were weighted by

195 precipitation amount to obtain representative mean values. Subsequently, correlation coefficients between δ^2H_{LM} tree-ring series and local climate parameters of Hohenpeißenberg were assessed for the common period of overlap (1916-2015) employing data of the nearby DWD weather station. To assess large-scale temperature influences on the Hohenpeißenberg tree-rings, spatial correlations between δ^2H_{LM} and the HadCRUT4.6 ensemble data (Morice et al., 2012) were conducted over the 1916-2015 period. Due to the prevailing westerlies

200 across Europe, we focused on areas mainly west of Hohenpeißenberg (~48 °N, 11 °E). Thus, spatial correlations with land and sea surface air temperature (CRU TS 4.01 and HadSST1, respectively) were conducted from North Africa to southern Scandinavia and from the Eastern North Atlantic to mid-Europe (range: 35 – 60°N and 30°W – 20°E) employing the KNMI climate explorer at 1° x 1° resolution (Royal Netherlands Meteorological Institute; http://climexp.knmi.nl). The reconstruction skill for δ^2H_{LM} tree-ring series and climate parameters was assessed

205 by the Durbin-Watson statistics (DW) testing for lag-1 autocorrelation in the linear model residuals.

4. Results and discussion

4.1 Intra- and inter-tree variability of the δ^2H_{LM} series

For the common period of overlap (1916-2015), maximum and minimum δ^2H_{LM} values of the nine tree-ring series ranged from –243 to –224 ‰ and –295 to –270 ‰, respectively, yielding maximum δ^2H_{LM} differences

210 within a core ranging between 41 and 66 ‰ (Table 2). Mean δ^2H_{LM} values ranged from –250 ± 8 to –271 ± 11 (±1σ standard deviation), whereby the magnitude of this range primarily results from δ^2H_{LM} differences among trees rather than between radii. Hence, in agreement with earlier findings (Anhäuser et al., 2017b; Riechelmann et al., 2017), δ^2H_{LM} values can differ regarding 'absolute' values particularly between trees by up to 21 ‰. Anhäuser et al. (2017b) suggested that about half of the inter-tree variability results from site-specific δ^2H

215 differences of the tree source water (i.e., δ^2H differences may already exist prior to water uptake), highlighting, however, that deviations in the biosynthetic isotope fractionation cannot be excluded.

Employing the full length of each of the nine tree-ring series, highly significant correlations (p < 0.001) can be noted among the δ^2H_{LM} series, whereby somewhat higher r values are observed within trees (ranging from 0.49 to 0.73) compared to inter-trees (ranging from 0.37 to 0.66; Table 3). Over the common period 1916-2015, inter-

220 series correlation (Rbar) yielded 0.52. Hence, even though δ^2H_{LM} values can differ regarding 'absolute' values particularly between trees by up to 21 ‰, the common variability indicates that these 'absolute' δ^2H_{LM} differences remain predominantly constant over time. Lag-1 is high and ranges between 0.40 and 0.78 indicating strong lag effects inherent to all δ^2H_{LM} series. These autocorrelations may reflect an autocorrelation adopted from the δ^2H_{precip} values. An equivalent autocorrelation for the δ^2H_{precip} over the 1971-2008 period cannot be

225 observed (r = 0.22, p > 0.1). However, a lack of autocorrelation in the δ^2H_{precip} data excludes not an absence of autocorrelation for δ^2H_{sw} values. Whereas δ^2H_{precip} values are individually measured of monthly collected precipitation, the source water δ^2H value reflects an integral of multiple precipitation events or even seasons reflecting a water body with a progressively changing δ^2H value. Thus, it seems (hydrologically) reasonable to assume an autocorrelation inherent to δ^2H_{sw} which is transferred to the δ^2H_{LM} tree-ring series. Nonetheless, the

230 autocorrelations observed for the δ^2H_{LM} tree-ring series may also point to some hydrogen 'storage effect' such as the incorporation of remobilized hydrogen during the lignin methoxyl groups biosynthesis.

To emphasize the coherent long-term δ^2H_{LM} variability of the four *Fagus sylvatica* trees, we calculated for each series the annual δ^2H_{LM} deviation to its mean value of the 1961-1990 period and averaged the resulting index δ^2H_{LM} series for each tree to produce four mean δ^2H_{LM} series (Fig. 3). For each mean series, both the short-term (inter-annual) and long-term (multi-decadal) changes in δ^2H_{LM} values are comparable in magnitude with up to ~20 ‰. The long-term δ^2H_{LM} trends can broadly be grouped into four phases including *(1)* a decline of ~20 ‰ from 1858-1916 (covered only by F2), *(2)* a ~15 ‰ increase from 1916-1956 retained in all tees, *(3)* a decrease of ~10 ‰ until 1981, and *(4)* an increase by ~25 ‰ during the most recent decades. The most recent increase in δ^2H_{LM} values is most pronounced in F4.

4.2 Assessment of tree age related influences on δ^2H_{LM} values and mean chronology development

δ^2H_{LM} values may additionally be affected by non-climatic influences related to age or tree height. To test for this, we compared linear fits among the four mean δ^2H_{LM} series using the 1916-1956 period (above described as phase two) as here each series shows a significant positive linear trend sharing also a common positive δ^2H_{LM} excursion at the end of the period (1956; Fig. 3b). Moreover, during this 51 years period, the four *Fagus sylvatica* trees reflect different age phases including a juvenile phase of F1 (cambial age 12-52), intermediate phases of F4 and F3 (cambial age 27-67 and 34-74, respectively) as well as a mature phase of F2 (cambial age 81-121). This allows a statistical assessment of differences among δ^2H_{LM} trends and tree age (cf. Table 4). The slopes of the linear regressions over the period 1916-1956 become steeper with decreasing tree age phase (0.24 ± 0.18, 0.34 ± 0.14, 0.31 ± 0.17 and 0.49 ± 0.18 ‰ per year; Table 4; Fig. 4). However, when conducting a two-tailed t-test for slope differences, only the linear fits of juvenile F1 data and the mature F2 data are statistically different at p < 0.1. Hence, the elevated slope of F1 compared to F2 suggests a juvenile effect of F1 associated with increasing δ^2H_{LM} values (0.25 ‰ per year). Even though statistically significant, the magnitude of this potential 'juvenile trend' falls notably below the inter-annual δ^2H_{LM} variability of up to 20 ‰ (Fig. 3) as well as the average analytical overall uncertainty of ± 3.6 ‰ and, thus, should have a negligible effect on the general coherency. A visibly stronger discrepancy in δ^2H_{LM} trends among the different trees can be observed for F4 at the end of our chronology (Fig. 3b). When comparing this discrepancy to F3, having a similar age as F4 (7 years apart; Table 1) suggests an influence not related to tree age. Consequently, deviations in the temporal δ^2H_{LM} trends seem not primarily associated with juvenile growth phases or tree age in general but may also be associated by temporal disturbances of δ^2H_{sw} among the four tree sampling sites, for instance, induced by changes in the source water accumulation. A better understanding of such occasional temporal trend deviations in δ^2H_{LM} may improve sampling strategies. Trees with potential temporal disturbances in the δ^2H_{sw}-δ^2H_{LM} relationship may justifiably be excluded when producing a mean δ^2H_{LM} chronology subsequently leading to an improved overall coherency.

For cellulose-derived δ^2H and $\delta^{18}O$ tree-ring series, there are commonly two mechanisms considered to induce juvenile trends. First, arid study sites with high evaporation rates may lead to an evaporative enrichment of heavier stable isotopes in source waters of upper soil layers (Allison, 1982; Hsieh et al., 1998; Kanner et al., 2014). In presence of such a gradient in stable water isotopes in soils, trees would use consecutively less ²H enriched soil waters over time as their root system progressively accesses deeper soil layers. Such a process would add a decreasing component to tree-ring δ^2H and $\delta^{18}O$ values until the root system is fully developed as has been suggested for a cellulose-derived $\delta^{18}O$ series from the Mediterranean (Corsica, France; Szymczak et al., 2012). Another mechanism for juvenile trends may be induced by a gradient of relative humidity under the forest

canopy. A decrease in relative humidity with height has been observed in temperate forests (Eliáš et al., 1989; Zweifel et al., 2002), which would intensify ^{18}O enrichment as leaf water evaporation rates increase with tree height (Labuhn et al., 2014). Hence, with increasing tree height (or age), leaf water would become gradually

275 more enriched in heavy stable water isotopes. Contrary to the first mechanism, such a process would lead to increasing δ²H and δ^{18}O values in juvenile tree-rings. However, for δ²H$_{LM}$ values, we consider only the first (soil water-related) mechanism as influential because leaf water-derived hydrogen is not involved in lignin methoxyl group's biosynthesis (Boerjan et al., 2003). Thus, as the juvenile δ²H$_{LM}$ values of F1 presented in this study show a minor mean trend deviation (associated with increasing δ²H values), this indicates no impact of soil water-

280 related juvenile effects, which would be associated with decreasing δ²H values. This may either point to a weak or nonexistent gradient of soil water δ²H values at Hohenpeißenberg or to a quickly developed root system of *Fagus sylvatica* trees within the first decade of growth. Nonetheless, future studies should take into account the potential influence of soil water evaporation rates on juvenile δ²H$_{LM}$ values, in particular for more arid study sites than Hohenpeißenberg. Furthermore, the most pronounced discrepancy in the temporal δ²H$_{LM}$ trend noted

285 for F4, which is presumably not age-related, highlights to investigate other non-climatic influences as well. A plausible mechanism would be a changing relationship between δ²H$_{precip}$ and δ²H of the source water over time in the nearby tree environment, such as changing soil and hydrological properties (leading to different source water accumulations).

We developed a chronology (without conducting any detrending or correction method) for the common period

290 1916-2015 by calculating for each of the nine tree-ring series the annual δ²H$_{LM}$ deviation to the mean of the 1961-1990 period. Subsequently, by integrating all nine δ²H$_{LM}$ series, a mean chronology was calculated with 95% confidence intervals to account for the interval variability (Fig. 5).

4.3 Relationship between δ²H$_{LM}$ chronology and δ²H$_{precip}$ as well as local and large-scale climate

The results clearly show that our mean δ²H$_{LM}$ chronology correlates best with weighted mean annual δ²H$_{precip}$

295 signatures using time periods such as January until December with r = 0.66 (p < 0.001; Fig. 6a) or previous September to current August with r = 0.73 (p < 0.001) when compared to seasonal and monthly δ²H$_{precip}$ signatures. The increased r value for the 'shifted' mean annual δ²H$_{precip}$ values agrees with the timing of early and late wood formation (growth season) and the source water accumulation. As tree-ring growth ceases in fall, precipitation falling after the latest late wood formation may only contribute to the tree source water of the

300 following year. Hence, in agreement with considerations in annual source water accumulation and tree-ring growth, the δ²H$_{LM}$ chronology is considered to reflect primarily mean annual δ²H$_{precip}$ values (previous September to current August) for the 1971-2008 period of data overlap. For the remaining years of the full 1916-2015 period, care has to be taken when the relative contribution of seasonal precipitation to the annual amount changes. In that case, δ²H$_{LM}$ would reflect a more seasonally pronounced δ²H$_{precip}$ signature. However, even

305 though this induces some noise into the δ²H$_{precip}$-δ²H$_{LM}$ relationship, we consider this influence as negligible for Hohenpeißenberg since neither annual nor seasonal precipitation amount changes significantly over 1916-2015 (cf. Sect. 2).

When comparing the δ²H$_{LM}$ chronology with temperature data of the nearby DWD station (covering the full period of 1916 - 2015), highly significant correlations (p < 0.001) are found for numerous months (previous

310 October, January, April, June, August) with r values ranging from 0.26 to 0.39 and for all seasons except for fall of the current year with r values ranging from 0.29 to 0.41 (Fig. 6b). Similar as observed for δ²H$_{precip}$, highest

correlation coefficients can, however, be noted for annually averaged temperatures with r = 0.53 (year defined from January to December) and r = 0.56 (year defined from previous September to August). Precipitation amount does not show any highly significant correlation to the δ^2H_{LM} chronology (Fig. 6b).

315   As indication was found that the δ^2H_{LM} chronology reflects best annually averaged δ^2H_{precip} values considering the year prior to the latest late wood formation, spatial correlations have been accordingly estimated between the mean δ^2H_{LM} chronology from Hohenpeißenberg (Germany) and mean annual surface air temperatures of previous September to current August. The results now significance across Western Europe (r ranging from 0.2 to >0.6; Fig. 7a). Highest correlations (with r > 0.6) are found for both land (northern Mediterranean) and sea

320   areas (western Mediterranean Sea, northwest North Sea, Gulf of Biscaya and parts of the eastern North Atlantic). This shows that the δ^2H_{LM} chronology exhibits higher correlations with temperature anomalies of multiple remote areas than with local temperature anomalies at Hohenpeißenberg (r = 0.56; Fig. 5b). To test the temporal robustness of the relationship between the δ^2H_{LM} chronology and Western European surface air temperatures, spatial correlations have also been determined for the 50-year periods 1916-1965 and 1966-2015 (cf. Fig. 7b and

325   C). Similarly as observed for the full period, the Hohenpeißenberg δ^2H_{LM} chronology and surface air temperature anomalies show significant correlations for both periods for large areas across western and central Europe. However, areas of highest correlations expand eastwards and increase in magnitude with time (cf. Fig. 7b and c). This leads particularly to an enlarged coverage of areas of high correlation for European land masses.

Besides changes in local temperature, δ^2H_{precip} at the site of precipitation is controlled by a number of large-scale

330   and remote hydro-climatic influences such as changing meteorological conditions in the moisture source area and meridional atmospheric transport particularly a modified water volume loss, but also potential mixing with different air masses (Araguas-Araguas et al., 2000; Dansgaard, 1964; Rozanski et al., 1993). The main moisture source of precipitation of the northern Alpine foothills (including the Hohenpeißenberg study site) has been determined by Lagrangian moisture source diagnostics for the time period 1995-2002 (Sodemann and Zubler,

335   2010). This study concludes that the majority of annual northern Alpine precipitation originates from multiple sources including the eastern North Atlantic (~29 %), the Western Mediterranean Sea (~16%), the North and Baltic Sea (~13 %) and continental Europe (~21 %). Consequently, even though our δ^2H_{LM} chronology shows highly significant correlations with large-scale and remote annual temperature changes, the involved stable water isotope mechanisms on Hohenpeißenberg δ^2H_{precip} values are more complex considering the multiple moisture

340   source areas of northern Alpine precipitation and the associated numerous hydro-climatic influences therein. Interestingly is, however, that northern Alpine moisture source areas overlap broadly with areas where surface air temperature changes show the highest correlations with the Hohenpeißenberg δ^2H_{LM} chronology (r between 0.5 and >0.6; Fig. 7a). The overlap of both these areas may suggest that temperature changes in the (remote) moisture source areas are an important control of the site-specific δ^2H_{precip} variance at Hohenpeißenberg.

345   Furthermore, applying this finding to the observed eastward expansion of areas of highest correlation from 1916-1965 to 1966-2015 may point to an eastward expansion of moisture source areas of northern Alpine precipitation during the 20th century (from the European shelf to Western and Central Europe).

4.3.1 econstructions of averaged western European surface air temperature changes

Even though areas of highest correlations between surface air temperatures and the δ^2H_{LM} chronology expand

350   eastwards with time, those areas are connected across Western Europe and overlap largely over time (Fig. 7). Hence, the δ^2H_{LM} chronology may be suitable to reconstruct average surface air temperatures of this large-scale

Climate
of the Past
Discussions

area (30 °W - 20 °E; 35 - 60 °N; area displayed in Fig. 7). To test this we developed a linear regression model
between the annually averaged (previous September to August) Western European surface air temperature
(WESAT) anomaly and the δ^2H_{LM} chronology yielding r = 0.71 (p < 0.001, DW = 1.6). When expressing the

355 linear regression model, the following equation is obtained:

$$\textbf{Eq. (1)}: \Delta\text{Temperature}_{WESAT}\ [°C] \approx (\Delta\delta^2H_{LM}\ [‰] + 0.98\ )\ /\ 15.88\ [‰\ /\ °C]$$

We subsequently compared the reconstructed and instrumental WESAT anomalies at annual resolution (Fig. 8).
To account for errors induced by the internal δ^2H_{LM} variability of the nine tree-ring series, we converted the
annually estimated 95% confidence interval (error bars in Fig. 5) into temperature using Eq. (1). As an additional

360 error assessment, we calculated the differences of the reconstructed and instrumental WESAT anomalies that
result at annual resolution and with a moving average of 5 (Fig. 8b). Differences between annually reconstructed
and instrumental WESAT anomalies differ in the range of Δ -0.9 to Δ 1.3 °C with an average absolute deviation
of 0.3 °C (n = 100) (Fig. 8b). Hence, for the broad majority of annual reconstructions (n = 84), absolute
deviations are < 0.5 °C, whereby the remaining absolute deviations in annual reconstructions are either between

365 0.5 and 1.0 (n = 14) and highest in 1956 and 1993. For the smoothed data (moving average of 5 data points), the
agreement between reconstructed and instrumental WESAT anomalies can particularly be observed for the main
part of our chronology (1937 - 2007), where absolute differences are entirely < 0.3 °C (Fig. 8b). Prior and after
this period, elevated absolute differences between the reconstructed and instrumental WESAT anomalies of up to
0.5 °C can occur for several consecutive years. These periods of elevated absolute differences broadly coincide

370 with the discrepancies in the decadal δ^2H_{LM} variability among the four *Fagus sylvatica* trees as noted for F1
(1916 – 1956) as well as for F4 (late 1990's – 2015) (Fig. 3b). Conclusively, despite the complex evolution of
northern Alpine δ^2H_{precip} changes, the δ^2H_{LM} chronology and the produced simple linear regression model
suggest that half of the variance (r² = 0.51) can be explained by large-scale annually averaged temperature
changes.

375 **5. Conclusions**

In this study, we investigated in detail the relationship between inter-annually resolved δ^2H_{LM} values and (site-
specific) instrumental δ^2H_{precip} as well as local and large-scale climate data by using nine annually resolved
Fagus sylvatica tree-ring series collected at Hohenpeißenberg (Germany). For the common period of overlap
(1916-2015), the coherency among the nine δ^2H_{LM} tree-ring series is indicated by high inter-series correlations

380 (Rbar = 0.52). However, some trees show partial deviations in their temporal δ^2H_{LM} trends, which, however,
seem neither be associated with known stable isotope mechanisms affecting juvenile tree-rings nor related to
specific tree ages in general. Nonetheless, the significant overall inter-series correlation gives confidence to
produce an averaged δ^2H_{LM} chronology (integrating the nine tree-ring series) subsequently being used to assess
co-variances with δ^2H_{precip} and climate parameters. Locally, the highest correlations between the δ^2H_{LM}

385 chronology were generally found with annually averaged values of δ^2H_{precip} (r = 0.73, p<0.001) and temperature
(r = 0.56, p <0.001) particularly when considering the year prior the latest late wood formation as, for instance,
from previous September to current August. Correlations with temperature further increased when compared to
large-scale temperature anomalies across Western Europe showing r values higher than 0.6 for multiple (largely
connected) are s. Those areas largely overlap with modern moisture source areas of the Hohenpeißenberg study

390 site indicating that remote meteorological changes primarily control the variance of the δ^2H_{LM} chronology. As

the δ^2H_{LM} chronology shows significant correlations with surface air temperatures for largely connected areas across western Europe (these areas also largely overlap over time), we produced a linear regression model between average surface air temperature anomalies of western Europe and the δ^2H_{LM} chronology (r = 0.71, p<0.1). When comparing instrumental and reconstructed large-scale temperature anomalies, an average absolute

395 deviation in annual reconstructions of 0.3 °C was found (n = 100). Therefore, δ^2H_{LM} values of mid-latitudinal tree-ring archives are considered suitable for reconstructions of large-scale mean annual temperature variability and may therefore particularly complement commonly used plant physiological tree-ring proxies (reflecting local temperature variability) yielding an improved paleoclimatic potential of Late Holocene tree-ring archives.

Data availability

400 The data used in this publication are available to the community and can be accessed by request to the corresponding author.

Author contributions

FK and TA designed the study. Financial support acquired by FK. BS and TA carried out field campaigns guided by WT. Tree-ring dating conducted by BS, CH and JE. BS, TA, FK and MG generated stable isotope data. TA,
405 CH, WT, DS, JS and FK interpreted the data and wrote the paper.

Competing interests

The authors declare no competing financial interests.

Acknowledgments

References

Allison, G. B.: The relationship between 18O and deuterium in water in sand columns undergoing evaporation, J. Hydrol., 55(1–4), 163–169, doi:10.1016/0022-1694(82)90127-5, 1982.
415 Anhäuser, T., Greule, M., Polag, D., Bowen, G. J. and Keppler, F.: Mean annual temperatures of mid-latitude regions derived from δ^2H values of wood lignin methoxyl groups and its implications for paleoclimate studies, Sci. Total Environ., 574, 1276–1282, doi:10.1016/j.scitotenv.2016.07.189, 2017a.
Anhäuser, T., Greule, M. and Keppler, F.: Stable hydrogen isotope values of lignin methoxyl groups of four tree species across Germany and their implication for temperature reconstruction, Sci. Total Environ., 579, 263–271,
420 doi:10.1016/j.scitotenv.2016.11.109, 2017b.
Anhäuser, T., Hook, B. A., Halfar, J., Greule, M. and Keppler, F.: Earliest Eocene cold period and polar amplification - Insights from δ2H values of lignin methoxyl groups of mummified wood, Palaeogeogr. Palaeoclimatol. Palaeoecol., 505(May), 326–336, doi:10.1016/j.palaeo.2018.05.049, 2018.
Araguas-Araguas, L., Froehlich, K. and Rozanski, K.: Deuterium and oxygen-18 isotope composition of precipitation and
425 atmoshperic moisture, Hydrol. Process., 14(July 1999), 1341–1355, doi:10.1002/1099-1085(20000615)14:8<1341::AID-HYP983>3.0.CO;2-Z, 2000.
Boerjan, W., Ralph, J. and Baucher, M.: Lignin Biosynthesis, Annu. Rev. Plant Biol., 54(1), 519–546, doi:10.1146/annurev.arplant.54.031902.134938, 2003.
Büntgen, U., Tegel, W., Nicolussi, K., McCormick, M., Frank, D., Trouet, V., Kaplan, J. O., Herzig, F., Heussner, K.-U.,

430 Wanner, H., Luterbacher, J. and Esper, J.: 2500 Years of European Climate Variability and Human Susceptibility, Science, 331(6017), 578–582, doi:10.1126/science.1197175, 2011.

Dansgaard, W.: Stable isotopes in precipitation, Tellus, 16(4), 436–468, doi:10.3402/tellusa.v16i4.8993, 1964.

Ehleringer, J. R. and Dawson, T. E.: Water uptake by plants: perspectives from stable isotope composition, Plant. Cell Environ., 15(9), 1073–1082, doi:10.1111/j.1365-3040.1992.tb01657.x, 1992.

435 Eliáš, P., Kratochvílová, I., Janouš, D., Marek, M. and Masarovičová, E.: Stand mircoclimate and physiological activity of tree leaves in an oak-hornbeam forest, Trees - Struct. Funct., 4, 227–233, 1989.

Esper, J., Cook, E. R. and Schweingruber, F. H.: Low-frequency signals in long tree-ring chronologies for reconstructing past temperature variability., Science, 295(March), 2250–2253, doi:10.1126/science.1066208, 2002.

Feakins, S. J., Ellsworth, P. V. and Sternberg, L. da S. L.: Lignin methoxyl hydrogen isotope ratios in a coastal ecosystem,
440 Geochim. Cosmochim. Acta, 121, 54–66, doi:10.1016/j.gca.2013.07.012, 2013.

Feng, X. H. and Epstein, S.: Climatic temperature records in delta-D data from tree-rings, Geochim. Cosmochim. Acta, 59(14), 3029–3037 [online] Available from: isi:A1995RL88800011, 1995.

Flanagan, L. B., Comstock, J. P. and Ehleringer, J. R.: Comparison of Modeled and Observed Environmental Influences on the Stable Oxygen and Hydrogen Isotope Composition of Leaf Water in Phaseolus vulgaris L., Plant Physiol., 96(2), 588–
445 596, doi:10.1104/pp.96.2.588, 1991.

Gärtner, H. and Nievergelt, D.: The core-microtome: A new tool for surface preparation on cores and time series analysis of varying cell parameters, Dendrochronologia, 28(2), 85–92, doi:10.1016/j.dendro.2009.09.002, 2010.

Gori, Y., Wehrens, R., Greule, M., Keppler, F., Ziller, L., La Porta, N. and Camin, F.: Carbon, hydrogen and oxygen stable isotope ratios of whole wood, cellulose and lignin methoxyl groups of Picea abies as climate proxies, Rapid Commun. Mass
450 Spectrom., 27(1), 265–275, doi:10.1002/rcm.6446, 2013.

Greule, M., Mosandl, A., Hamilton, J. T. G. and Keppler, F.: A rapid and precise method for determination of D/H ratios of plant methoxyl groups, Rapid Commun. Mass Spectrom., 22, 3983–3988, doi:DOI: 10.1002/rcm.3817, 2008.

Hartl-Meier, C., Zang, C., Büntgen, U., Esper, J., Rothe, A., Göttlein, A., Dirnböck, T. and Treydte, K.: Uniform climate sensitivity in tree-ring stable isotopes across species and sites in a mid-latitude temperate forest, Tree Physiol., 35(1), 4–15,
455 doi:10.1093/treephys/tpu096, 2014.

Holmes, R. L.: Computer-assisted quality control in tree-ring dating and measurement, Tree Ring Bull., 43(1), 69–78, doi:10.1016/j.ecoleng.2008.01.004, 1983.

Hsieh, J. C. C., Chadwick, O. A., Kelly, E. F. and Savin, S. M.: Oxygen isotopic composition of soil water: Quantifying evaporation and transpiration, Geoderma, 82(1–3), 269–293, doi:10.1016/S0016-7061(97)00105-5, 1998.

460 Kanner, L. C., Buenning, N. H., Stott, L. D., Timmermann, A. and Noone, D.: The role of soil processes in δ18O terrestrial climate proxies, Global Biogeochem. Cycles, 28, 239–252, doi:10.1002/2013GB004742, 2014.

Keppler, F., Harper, D. B., Kalin, R. M., Meier-Augenstein, W., Farmer, N., Davis, S., Schmidt, H. L., Brown, D. M. and Hamilton, J. T. G.: Stable hydrogen isotope ratios of lignin methoxyl groups as a paleoclimate proxy and constraint of the geographical origin of wood, New Phytol., 176(3), 600–609, doi:10.1111/j.1469-8137.2007.02213.x, 2007.

465 Labuhn, I., Daux, V., Pierre, M., Stievenard, M., Girardclos, O., Féron, A., Genty, D., Masson-Delmotte, V. and Mestre, O.: Tree age, site and climate controls on tree ring cellulose δ18O: A case study on oak trees from south-western France, Dendrochronologia, 32(1), 78–89, doi:10.1016/j.dendro.2013.11.001, 2014.

Liu, X., An, W., Treydte, K., Wang, W., Xu, G., Zeng, X., Wu, G., Wang, B. and Zhang, X.: Pooled versus separate tree-ring δD measurements, and implications for reconstruction of the Arctic Oscillation in northwestern China, Sci. Total Environ.,
470 511, 584–594, doi:10.1016/j.scitotenv.2015.01.002, 2015.

Mann, M. E., Bradley, R. S. and Hughes, M. K.: Global-scale temperature patterns and climate forcing over the past six centuries, Nature, 392(6678), 779–787, doi:10.1038/33859, 1998.

McCarroll, D. and Loader, N. J.: Stable isotopes in tree rings, Quat. Sci. Rev., 23(7–8), 771–801, doi:10.1016/j.quascirev.2003.06.017, 2004.

475 Mischel, M., Esper, J., Keppler, F., Greule, M. and Werner, W.: δ2H, δ13C and δ18O from whole wood, α-cellulose and lignin methoxyl groups in Pinus sylvestris: a multi-parameter approach, Isotopes Environ. Health Stud., 51(4), 553–568, 2015.

Morice, C. P., Kennedy, J. J., Rayner, N. A. and Jones, P. D.: Quantifying uncertainties in global and regional temperature change using an ensemble of observational estimates: The HadCRUT4 data set, J. Geophys. Res. Atmos., 117(8), 1–22,
480 doi:10.1029/2011JD017187, 2012.

Paul, D., Grzegorz, S. and Fórizs, I.: Normalization of measured stable isotopic compositions to isotope reference scales - a review, Rapid Commun. Mass Spectrom., 21, 3006–3014, 2007.

Pauly, M., Helle, G., Miramont, C., Büntgen, U., Treydte, K., Reinig, F., Guibal, F., Sivan, O., Heinrich, I., Riedel, F., Kromer, B., Balanzategui, D., Wacker, L., Sookdeo, A. and Brauer, A.: Subfossil trees suggest enhanced Mediterranean
485 hydroclimate variability at the onset of the Younger Dryas, Sci. Rep., 8(1), 13980, doi:10.1038/s41598-018-32251-2, 2018.

Riechelmann, D. F. C., Greule, M., Siegwolf, R. T. W., Anhäuser, T., Esper, J. and Keppler, F.: Warm season precipitation signal in δ 2 H values of wood lignin methoxyl groups from high elevation larch trees in Switzerland, Rapid Commun. Mass Spectrom., 31(19), 1589–1598, doi:10.1002/rcm.7938, 2017.

Roden, J. S., Lin, G. and Ehleringer, J. R.: A mechanistic model for interpretation of hydrogen and oxygen isotope ratios in
490 tree-ring cellulose, Geochim. Cosmochim. Acta, 64(1), 21–35, 2000.

Rozanski, K., Araguás-Araguás, L. and Gonfiantini, R.: Isotopic Patterns in Modern Global Precipitation, Clim. Chang. Cont. Isot. Rec., 78, 1–36, doi:10.1029/GM078p0001, 1993.

Sodemann, H. and Zubler, E.: Seasonal and inter-annual variability of the moisture sources for alpine precipitation during 1995-2002, Int. J. Climatol., 30(7), 947–961, doi:10.1002/joc.1932, 2010.

495 Sternberg, L. D. S. L. O. R.: Oxygen stable isotope ratios of tree-ring cellulose: The next phase of understanding, New Phytol., 181(3), 553–562, doi:10.1111/j.1469-8137.2008.02661.x, 2009.

Szymczak, S., Joachimski, M. M., Bräuning, A., Hetzer, T. and Kuhlemann, J.: Are pooled tree ring δ13C and δ18O series

Climate
of the Past

Discussions

Open Access

EGU

reliable climate archives? - A case study of Pinus nigra spp. laricio (Corsica/France), Chem. Geol., 308–309, 40–49, doi:10.1016/j.chemgeo.2012.03.013, 2012.

500   Tang, K., Feng, X. and Ettl, G. J.: The variations in δD of tree rings and the implications for climatic reconstruction, Geochim. Cosmochim. Acta, 64(10), 1663–1673, doi:10.1016/S0016-7037(00)00348-3, 2000.

Treydte, K. S., Schleser, G. H., Helle, G., Frank, D. C., Winiger, M., Haug, G. H. and Esper, J.: The twentieth century was the wettest period in northern Pakistan over the past millennium., Nature, 440(7088), 1179–1182, doi:10.1038/nature04743, 2006.

505   Zweifel, R., Böhm, J. P. and Häsler, R.: Midday stomatal closure in Norway spruce--reactions in the upper and lower crown, Tree Physiol., 22(15–16), 1125–1136, doi:10.1093/treephys/22.15-16.1125, 2002.

Table 1 – Age coverage of the nine tree-rings of *Fagus Sylvativa*

Series ID	Pith offset	First year	Last year
F1.1	7	1912	2015
F1.2	0	1905	2015
F1.3	7	1912	2015
F2.1	23	1858	2015
F2.2	8	1844	2015
F3.1	7	1890	2015
F3.2	33	1916	2015
F4.1	6	1896	2015
F4.2	26	1916	2015

Climate
of the Past
Discussions

Open Access

EGU

510   **Table 2** – Descriptive statistics of the nine $\delta^2 H_{LM}$ tree-ring series of the four *Fagus sylvativa* trees

| Series ID | $\delta^2 H_{LM}$ [‰ vs. VSMOW] over 1916-2015 | | | | |
	Minimum	Maximum	Difference (Max. − Min.)	Mean with SD (1σ)	Lag-1
F1.1	−294	−243	51	−269 ± 11	0.645
F1.2	−288	−243	45	−266 ± 10	0.515
F1.3[a]	−295	−236	59	−271 ± 11	0.408
F2.1	−270	−228	43	−250 ± 8	0.495
F2.2	−287	−224	63	−251 ± 8	0.782
F3.1	−279	−231	48	−251 ± 8	0.473
F3.2	−293	−227	66	−252 ± 13	0.598
F4.1	−277	−231	46	−261 ± 11	0.653
F4.2	−272	−231	41	−261 ± 15	0.718

[a]Nine years (1923-1931) are missing due to analytical problems

Table 3 – Peason's r (with n) between the nine annually resolved δ^2H_{LM} tree-ring series (all statistically significant at p < 0.001). Color shading indicates r values between radii of the same tree.

r / n	F1.1	F1.2	F1.3	F2.1	F2.2	F3.1	F3.2	F4.1	F4.2
F1.1		0.65	0.67	0.52	0.65	0.66	0.37	0.43	0.49
F1.2	104		0.69	0.49	0.61	0.63	0.59	0.55	0.59
F1.3	95	95		0.59	0.51	0.52	0.51	0.56	0.47
F2.1	104	104	95		0.49	0.40	0.40	0.42	0.37
F2.2	104	104	95	158		0.63	0.53	0.65	0.66
F3.1	100	100	91	100	100		0.59	0.51	0.54
F3.2	100	100	91	100	100	100		0.56	0.59
F4.1	100	100	91	100	100	100	100		0.73
F4.2	100	100	91	100	100	100	100	100	

Table 4 - Statistics of the linear regression analysis of the four mean $\delta^2 H_{LM}$ tree-ring series over the period 1916-1956 (as
515   shown in Fig. 4). Series are ordered in accordance to reflected growth phase.

Series	r (p<0.05)	Slope with 95 % CI [‰/year]	Cambial age covered
F2	0.39	0.24 ± 0.18	81 - 121 (mature)
F3	0.63	0.34 ± 0.14	34 - 74 (intermediate)
F4	0.50	0.31 ± 0.17	27 - 67 (intermediate)
F1	0.67	0.49 ± 0.18	12 - 52 (juvenile)

Fig. 1 – Map of the investigation area. Top left shows the location of the sampling site Hohenpeißenberg (white star) in
Germany. Circles in the aerial picture mark the location of the four *Fagus sylvatica* L. specimens (F1-F4) used for tree ring
δ^2H_{LM} measurements which are within a distance of 2 km from the Deutsche Wetterdienst (DWD) and the Global Network of
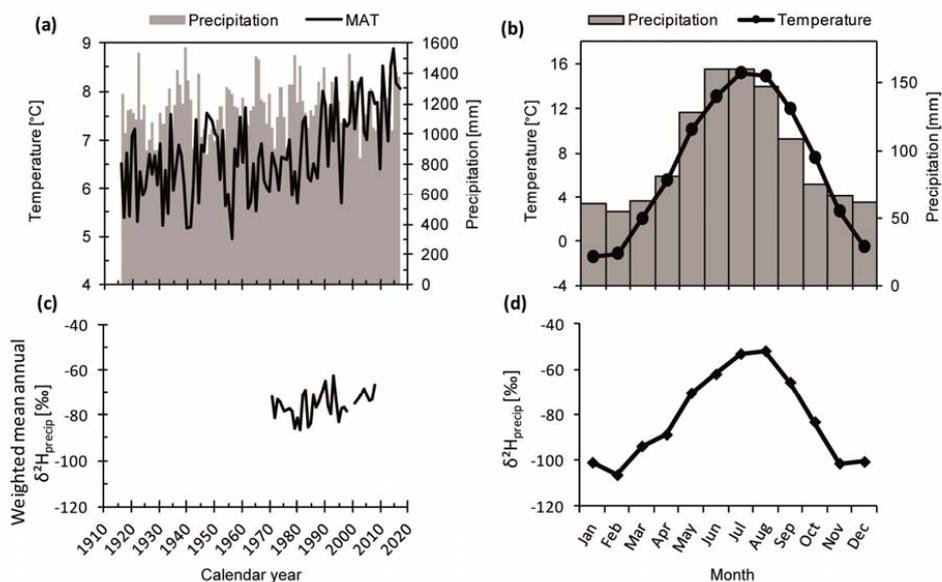520 Isotopes in Precipitation (GNIP) stations (square).

Fig. 2 – Instrumental climate and δ^2H_{precip} data from the DWD and GNIP stations at Hohenpeißenberg. **(a)** Mean annual temperature (MAT) and total precipitation since 1916. **(b)** Seasonal temperature and precipitation patterns over the 1916-2015 period. **(c)** Weighted mean annual δ^2H_{precip} values for the 1971-2008 period (the years 1999 and 2000 are missing due to insufficient data). **(d)** Monthly resolved mean δ^2H_{precip} values for the 1971-2008 period.
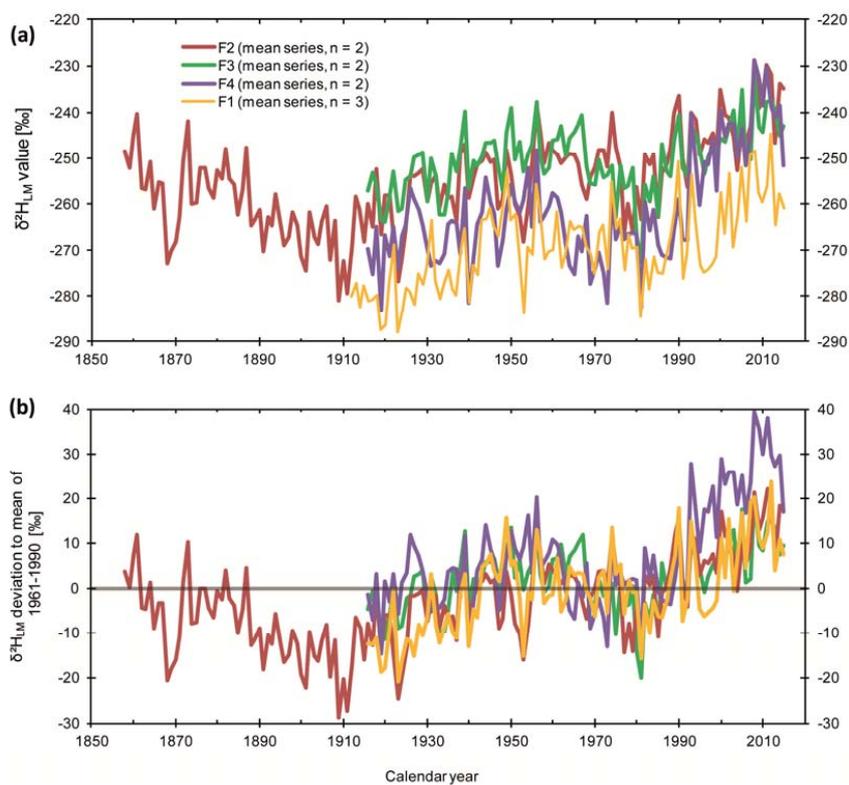
**Fig. 3 – (a)** Annually resolved δ^2H_{LM} values of the four *Fagus Sylvatica* trees (F1, F2, F3 and F4) collected at Hohenpeißenberg (Germany). Each series reflects the mean δ^2H_{LM} value of n = 2 or 3. **(b)** Standardized tree-ring series of (a) using the mean δ^2H_{LM} value of the reference period 1961-1990.

Climate
of the Past

Open Access

Discussions

EGU
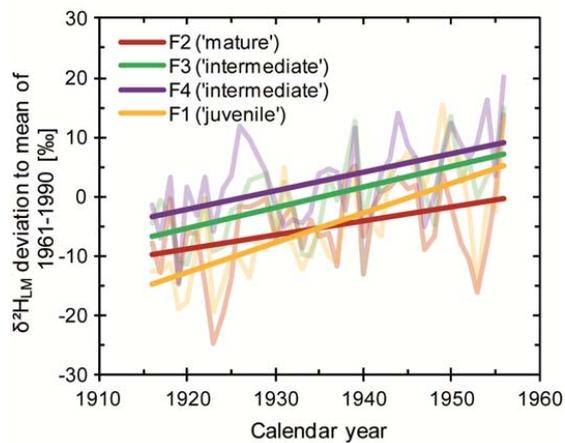
530

Fig. 4 – Linear regression analysis of the four mean δ²H$_{LM}$ tree-ring series over the period 1916-1956. During this period, trees differ in age. Statistics of linear fits are given in Table 4.
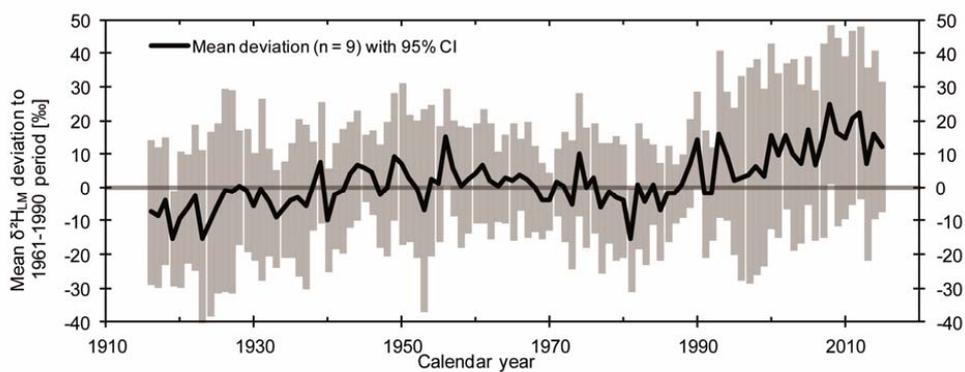
Fig. 5 – $\delta^2 H_{LM}$ chronology for the 1916-2015 common period. Chronology reflects the arithmetic mean of the annual $\delta^2 H_{LM}$
deviations with respect to the 1961-1990 period of the nine individual tree-ring series and is shown with 95 % confidence
intervals (grey bars).

Climate
of the Past
Discussions

Open Access
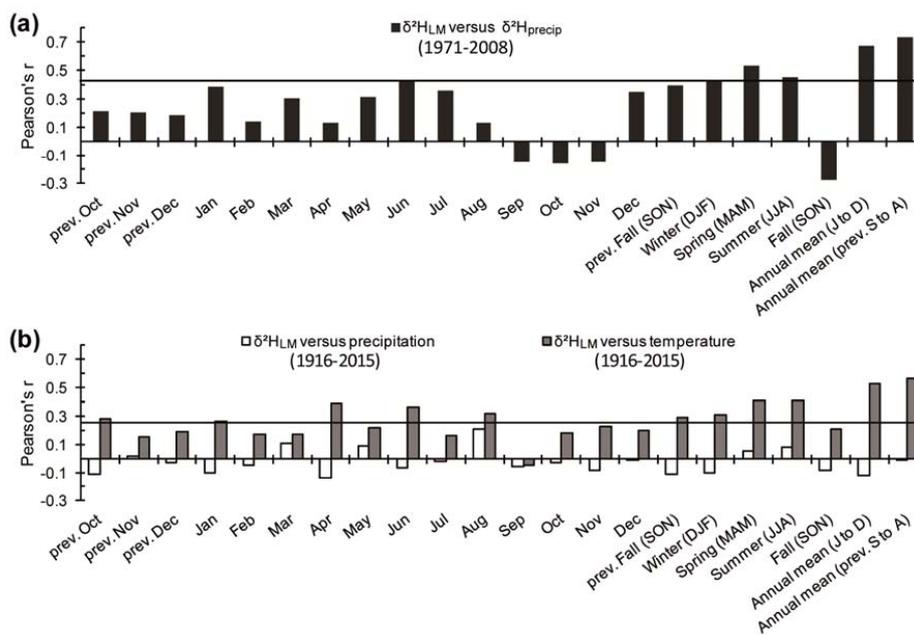
Fig. 6 - Pearson's correlations (r) between annually resolved mean δ^2H_{LM} chronology (cf. Fig. 5) and δ^2H_{precip} from 1971 – 2008 (n = 36) (**a**) as well as with temperature and precipitation from 1916-2015 (n = 100) (**b**) for Hohenpeißenberg (Germany). Horizontal lines mark significance level of 99.9%.

540
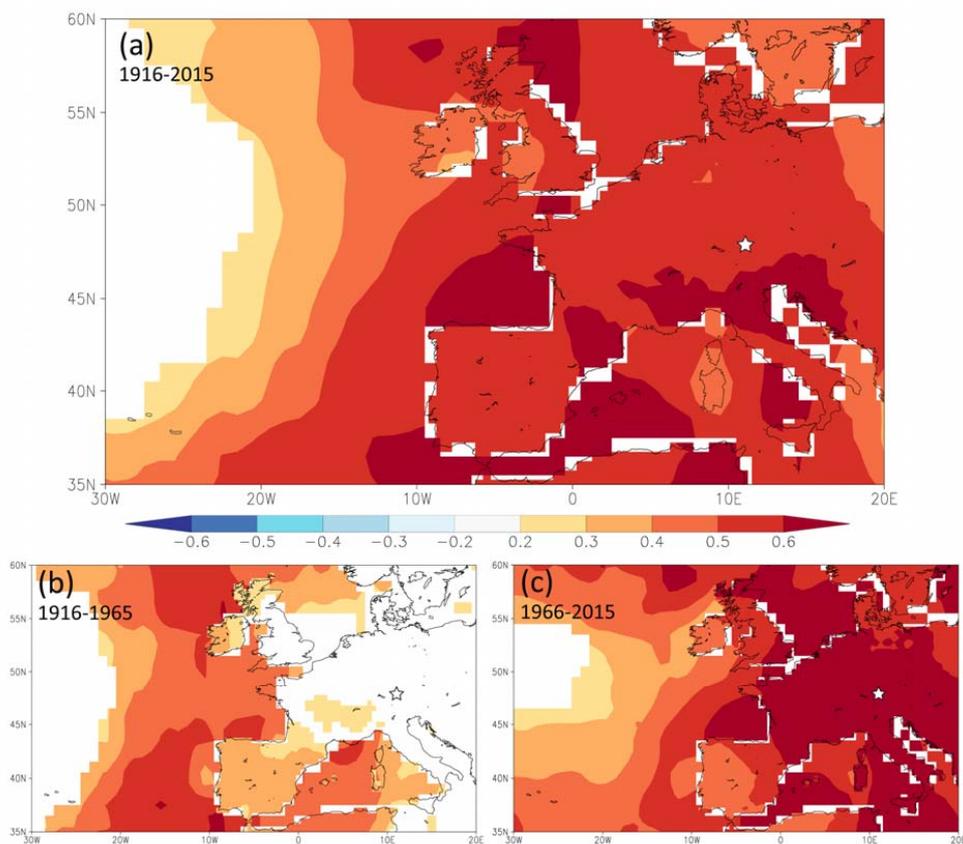
Fig. 7 – Spatial correlations between inter-annually resolved land and sea air temperature changes (previous September to current August; CRUT4.01 and HadSST1, respectively) and mean δ^2H_{LM} chronology from Hohenpeißenberg (Germany) for the time period 1916-2015 (**a**) as well as for the time periods 1916-1965 (**b**) and 1966-2015 (**c**). Only correlations with significance $p < 0.1$ are shown. White stars mark the Hohenpeißenberg study site in Germany.

Climate
of the Past
Discussions

Open Access

EGU
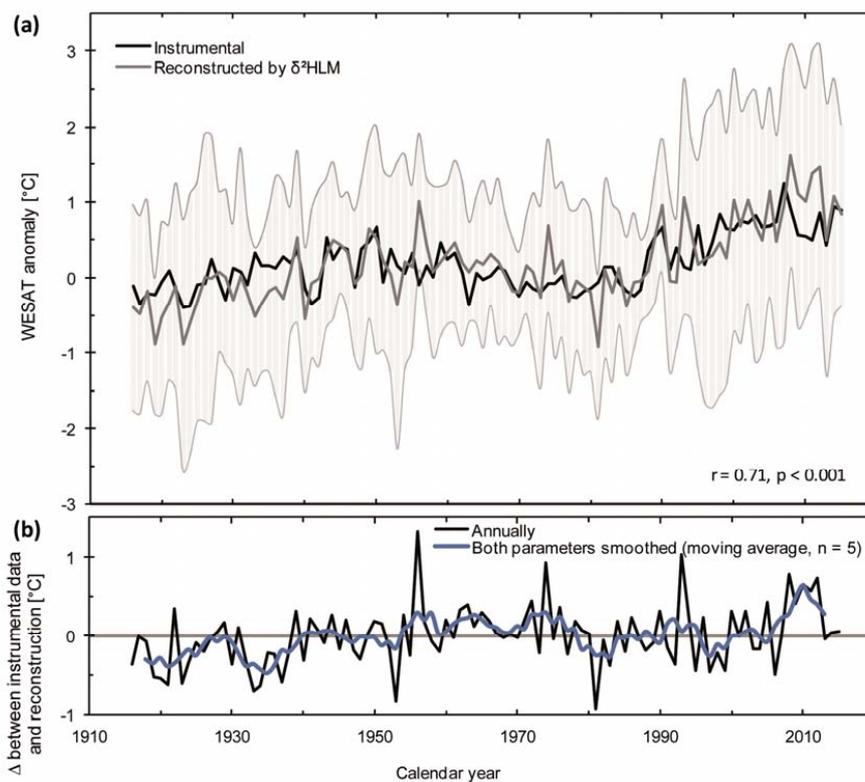
Fig. 8 – a) Instrumental and reconstructed WESAT anomaly (using Eq. (1)) for the time period 1916-2015 at annual
resolution. Equation (1) was also used to convert the annually estimated 95% confidence interval into temperature (grey bars)
to account for errors induced by the internal $\delta^2 H_{LM}$ variability of the nine tree-ring series **b)** Difference between reconstructed
550   and instrumental WESAT anomaly at annual resolution and with a moving average of 5 of both parameters.